applied sciences

MDPI

Article

Half-Spectrum Suppression in Dynamic Resonant Tunneling

Gilad Zangwill * and Er'el Granot *

Department of Electrical and Electronics Engineering, Ariel Photonic Center, Ariel University, Ariel 40700, Israel
* Correspondence: gzangwill@gmail.com (G.Z.); erel@ariel.ac.il (E.G.)

Abstract: It is well known that in a process of Dynamic Resonant Tunneling, where the energy level of the quasi-bound state varies in time, the tunneling current can be drastically suppressed at specific energies. These energies obey a generic quantization rule (QR). However, these systems exhibit two types of current suppression. In the first type, the current vanishes completely, and in the second the current is suppressed but does not vanish. We investigate these two types of current suppression and their relations to the quantization rule.

Keywords: resonant tunneling; quantum dynamics; dynamic resonant tunneling; suppression of tunneling; coherent destruction of tunneling; total reflection; Fano resonance; quasi-bound state

1. Introduction

The subject of tunneling suppression has been studied for decades. It has been shown that the tunneling current between two wells can be totally suppressed [1,2]. This finding was surprising not only due to its counter-intuitiveness, but also since it contradicts previously reported behavior of a similar system [3,4]. Later on, it was presented in a simple two-level solvable system [5,6]. At about the same time, it was shown that an oscillating delta function potential at certain energies shows zero transmission [7]. A similar phenomenon was found in more complex systems, such as in Dynamic Resonant Tunneling (DRT) processes (see Figure 1); recently, it was shown that zero transmission appears under certain conditions in dynamic tunneling processes [8]. The current paper shows that zero transmission can only appear when half of the spectrum is completely suppressed. Again, this was counter-intuitive, since it was anticipated that due to the high sensitivity of resonant tunneling current on the system's parameters, any spectrum widening would improve the probability of penetrating the opaque barrier. Indeed, many studies showed both experimentally and theoretically that oscillations and potential variations increase tunneling probability [9–17]. However, when the resonant level varies in time, at certain incoming particle energies, which obey a quantization rule, the tunneling current is highly suppressed [18–23]. Despite the fact that these quantization rules show a high agreement with exact numerical analysis, since these criteria are approximate analytical expressions, it is not clear whether they predict a criterion for complete suppression, i.e., zero current, or if they predict significant suppression, albeit where the current does not vanish.

Recently, it has been shown that DRT can be analyzed similarly to a stationary RT process [22]. In an RT process, the particle tunnels via a quasi-bound state (QBS), which is created due to the presence of a well inside the barrier. When the incoming particle's energy (Ω) matches the resonance energy $\Omega = \Omega_R$, transmission is high, while when there is no match the tunneling current is suppressed drastically. In a DRT process, the well oscillates, and therefore the QBS turns into a Quasi-Bound-Super-State (QBSS), which consists of an infinite array of coupled sub-states. Therefore, in accordance with the stationary model, when the incoming particle energy agrees with that of the sub-state energies, whose spectral component is high, the entire QBSS is excited and the total tunneling current is high, while when there is no match, the current is suppressed. That is, if $|\Phi_{QB}\rangle$ represents the QBSS,

check for updates

Citation: Zangwill, G.; Granot, E. Half-Spectrum Suppression in Dynamic Resonant Tunneling. *Appl. Sci.* **2023**, *13*, 12919. https://doi.org/10.3390/app132312919

Received: 30 September 2023
Revised: 26 November 2023
Accepted: 29 November 2023
Published: 2 December 2023

Copyright: © 2023 by the authors. Licensee MDPI, Basel, Switzerland. This article is an open access article distributed under the terms and conditions of the Creative Commons Attribution (CC BY) license (https://creativecommons.org/licenses/by/4.0/).

then therefore the probability of an incoming particle with energy Ω tunneling out with energy Ω_{out} is

$$p_{\Omega_{in},\Omega_{out}} \sim \left|\langle\Omega|\Phi_{QB}\rangle\right|^2 \left|\langle\Phi_{QB}|\Omega_{out}\rangle\right|^2 \tag{1}$$

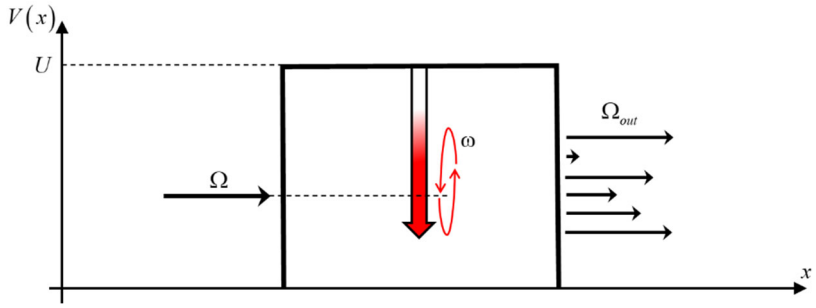


Figure 1. The system under study. An energetic particle tunnels through an opaque barrier with an oscillating well at its center. The red area inside the thick arrow (the well) represents the spectral width of the generated spectrum. The well oscillates with frequency ω (red arrow). U is the barrier height, Ω is the incoming energy, and Ω_{out} are the outgoing energies (arrows' length indicates different transmission probabilities).

When the well oscillates harmonically, the incoming particle can gain or lose energy quanta. Consequently, the spectrum of the particle consists only of discrete energy levels. Therefore, this model is useful when there is an agreement between $\langle\Omega_R\rangle$ (the mean value of the varying resonance energy level) and one of the particle's discrete spectral components. In this case, the QBSS $|\Phi_{QB}\rangle$ is well-defined, and its spectrum consists of the discrete levels

$$E_n = \langle\Omega_R\rangle + n\omega \tag{2}$$

where ω is the well's oscillating frequency, n is an integer and $\langle\Omega_R\rangle \equiv (\omega/2\pi)\int_0^{2\pi/\omega} \Omega_R(t)dt$ is the mean resonance energy level. In which case, if the component $\left|\langle\Omega|\Phi_{QB}\rangle\right|$ is high, the current is high, and when it is low the current is low as well. This model was used to investigate the dependence of the current's sensitivity on the incoming particle's energy. In particular, it explains the current suppression at certain energies [22]; however, it cannot predict the energies for which the current vanishes completely. When $\Omega = E_n$, the current can be suppressed by orders of magnitude but cannot reach zero. This behavior can be explained below.

When the well's energy varies in time, the resonance level varies as well: $\Omega_R(t)$. It has been shown that when the incoming energy solves the following equation,

$$\frac{1}{2}\int_{t_1}^{t_2} \left|\Omega - \Omega_R(t')\right| dt' = \pi\left(n - \frac{1}{4}\right) \tag{3}$$

where $\Omega_R(t)$ is the instantaneous resonant energy, $t_{1,2}$ are the solutions of $\Omega_R(t_{1,2}) = \Omega$ and n is a positive integer, the current is considerably suppressed [23]. In cases where the well's energy levels varies, like a hill, i.e., initially it increases and eventually decreases (or vice versa), Equation (3) shows the high prediction of full current suppression. In this category, one can include Gaussian, Secant and even Lorentzian perturbations. In all these cases, the resonance energy $\Omega_R(t)$ crosses the incoming particle's energy Ω exactly twice and therefore the instances $t_{1,2}$ are well defined (see the left panel of Figure 2).

However, in the case where the well oscillates harmonically, then in every period there are two extrema—one minimum and one maximum (see the right panel of Figure 2). Now,

if $\Omega = E_n$, then the same criterion (3) can be applied for both minima and maxima. In that case, then

$$\frac{1}{2}\int_{\tau}^{\tau+2\pi/\omega}\left[\Omega - \Omega_R(t')\right]dt' = \frac{\pi}{\omega}(\Omega - \langle\Omega_R\rangle) = n\pi \tag{4}$$

for any τ. Therefore, if

$$\frac{1}{2}\int_{t_1}^{t_2}\left|\Omega - \Omega_R(t')\right|dt' = \pi\left(n_1 - \frac{1}{4}\right) \tag{5}$$

then

$$\frac{1}{2}\int_{t_2}^{t_1+2\pi/\omega}\left|\Omega - \Omega_R(t')\right|dt' = \pi\left(n_2 - \frac{1}{4}\right) \tag{6}$$

where $n_2 = n + n_1$, since, without loss of generality $\Omega > \Omega_R(t)$ for $t_2 < t < t_1 + 2\pi/\omega$, then $\Omega < \Omega_R(t)$ for $t_1 < t < t_2$,

$$\frac{1}{2}\int_{t_2}^{t_1+2\pi/\omega}\left|\Omega - \Omega_R(t')\right|dt' = \frac{1}{2}\int_{t_1}^{t_1+2\pi/\omega}\left[\Omega - \Omega_R(t')\right]dt' + \frac{1}{2}\int_{t_1}^{t_2}\left|\Omega - \Omega_R(t')\right|dt' = \pi\left(n + n_1 - \frac{1}{4}\right) \tag{7}$$

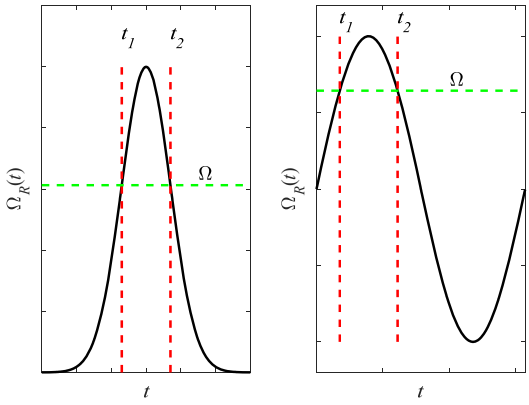


Figure 2. Temporal variations of the resonance energy level. **Left panel**: The resonance level varies like a Gaussian perturbation and crosses the particle energy twice (only one extremum). **Right panel**: The resonance level varies periodically. In every period there are two extrema.

It should be noted that in (4) n can be any integer, while n_1 and n_2 must be positive integers.

The same reasoning, of course, applies to high currents. If a high-current criterion is valid in the $t_1 < t < t_2$ domain, i.e.,

$$\frac{1}{2}\int_{t_1}^{t_2}\left|\Omega - \Omega_R(t')\right|dt' = \pi\left(n_1 + \frac{1}{4}\right) \tag{8}$$

then in the case where $\Omega = E_n$ a high current criterion is valid in the $t_2 < t < t_1 + 2\pi/\omega$ domain as well, i.e.,

$$\frac{1}{2}\int_{t_2}^{t_1+2\pi/\omega}\left|\Omega - \Omega_R(t')\right|dt' = \pi\left(n_2 + \frac{1}{4}\right) \tag{9}$$

Therefore, when $\Omega = E_n$ there is a consistency between the two parts of the period. Consequently, when $\Omega = E_n$, the QBSS in DRT behaves like a QBS in a stationary RT process—there is a clear criterion for maximum current and a clear criterion for current suppression. It is clear that (2) and (8) are the two required criteria to achieve the maximum current. However, it is also clear that despite the fact that (2) and (3) are criteria for current suppression, they cannot be sufficient for zero current (Fano resonances [8,24–31]). The reason is that like the stationary scenario, the transmission at the minima is not zero. Even in off-resonance cases some particles penetrate the barrier into the well and escape from the well across the barrier.

To generate a scenario of zero transmission, i.e., zero current, one must demand suppression criterion in only one part of the period. In this case, the entire spectrum is suppressed but half of it can go to zero. If, without loss of generality, we again take $\Omega > \Omega_R(t)$ for $t_2 < t < t_1 + 2\pi/\omega$ (and $\Omega < \Omega_R(t)$ for $t_1 < t < t_2$) and we further take the suppression criterion for $t_1 < t < t_2$ and current-enhancement criterion for $t_2 < t < t_1 + 2\pi/\omega$, then both (5) and (9) must be valid simultaneously. In this case,

$$\begin{aligned} \frac{\pi}{\omega}(\Omega - \langle\Omega_R\rangle) &= \tfrac{1}{2}\int_{t_1}^{t_1+2\pi/\omega} [\Omega - \Omega_R(t')]dt' \\ &= -\tfrac{1}{2}\int_{t_1}^{t_2} |\Omega - \Omega_R(t')|dt' + \tfrac{1}{2}\int_{t_2}^{t_1+2\pi/\omega} |\Omega - \Omega_R(t')|dt' = \pi\Big((n_2 - n_1) + \tfrac{1}{2}\Big) \end{aligned} \tag{10}$$

Therefore, this specific scenario can occur only between the QBSS energy levels, i.e., when

$$\Omega = E_{n+1/2} = \langle\Omega_R\rangle + \left(n + \frac{1}{2}\right)\omega \tag{11}$$

where in this case $n = n_2 - n_1$.

Clearly, the same conclusion appears when the suppression criterion is applied for the $t_2 < t < t_1 + 2\pi/\omega$ part, and current enhancement for the $t_1 < t < t_2$ part.

Below, we will investigate these cases. We will show that in the unique scenarios where the incoming particle energy is exactly between the QBSS sub levels, i.e., $\Omega = E_{n+1/2} = \langle\Omega_R\rangle + (n + 1/2)\omega$, and (5) or (6) (but not both) holds, then the spectrum is split into two. Both are suppressed, but half is suppressed to zero (see Figure 3). Consequently, if the suppressed part is the high-energy one, and the incoming energy is lower than the oscillating frequency, then the current reaches zero.

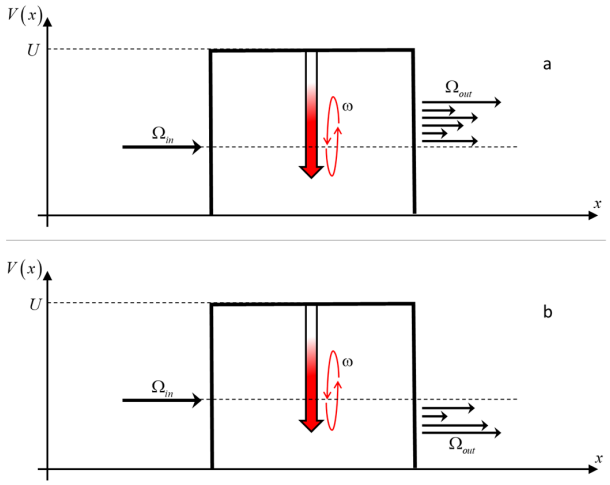


Figure 3. Upper panel (**a**): the system fulfills the criterion which completely suppresses the lower part of the spectrum. Lower panel (**b**): the higher part of the spectrum is completely suppressed.

2. The Model and Its Dynamics

The system is presented in Figure 1. A particle with energy Ω penetrates an opaque barrier. In the center of the barrier there is an oscillating well. For simplicity, the well is presented by a delta function; however, this is a very good approximation for the case where the well is considerably narrower than the particle's de Broglie wavelength [32].

The Schrodinger equation of this system reads

$$i\frac{\partial\psi}{\partial t} = -\frac{\partial^2}{\partial x^2}\psi + V(x)\psi + (\alpha + \beta\cos\omega t)\delta(x)\psi \tag{12}$$

where the units were taken for convenience considering that Planck's constant is $\hbar = 1$ and the particle's mass is $m = 1/2$, and

$$V(x) = \begin{cases} U & |x| < L \\ 0 & else \end{cases} \tag{13}$$

In this case, for a very wide barrier, the instantaneous resonance level can be written as follows [23]:

$$\Omega_R(t) \cong U - \frac{1}{4}(\alpha + \beta\cos\omega t)^2 \tag{14}$$

Equation (14) is accurate only when the barrier is infinitely wide.

Therefore, the mean resonance energy level, which is the QBSS spectrum's central energy, is

$$\langle\Omega_R(t)\rangle \cong U - \frac{1}{4}\left(\alpha^2 + \beta^2/2\right) \tag{15}$$

Due to the symmetry, current suppression occurs when either

$$\int_0^{t_1} \left|\Omega - \Omega_R(t')\right| dt' = \pi\left(n_1 - \frac{1}{4}\right) \tag{16}$$

or

$$\int_{t_1}^{\pi/\omega} \left|\Omega - \Omega_R(t')\right| dt' = \pi\left(n_2 - \frac{1}{4}\right) \tag{17}$$

where in this case

$$t_1 = \frac{1}{\omega}\arccos\left(\frac{2\sqrt{U-\Omega} - \alpha}{\beta}\right) \tag{18}$$

3. Exact Numerical Solution

The solution of Equation (12) can be written as a superposition of plane waves with discrete energies, i.e.,

$$\psi(x,t) = \begin{cases} \varphi_0^+ \exp(-i\Omega_0 t) + \sum\limits_{n=-\infty}^{\infty} r_n \varphi_n^- \exp(-i\Omega_n t) & x < 0 \\ \sum\limits_{n=-\infty}^{\infty} t_n \varphi_n^+ \exp(-i\Omega_n t) & x > 0 \end{cases} \tag{19}$$

where $\varphi_n^{\pm}$ are the homogeneous solutions for waves that propagate from left to right (φ_n^+) and from right to left (φ_n^-), namely

$$-\frac{\partial^2}{\partial x^2}\varphi_n^{\pm}(x) + [V(x) - \Omega_n]\varphi_n^{\pm}(x) = 0 \tag{20}$$

and

$$\varphi_n^+ \to \tau_{\Omega_n}\exp[ik_n x - i\Omega_n t] \ (for\ x \to \infty) \tag{21}$$

$$\varphi_n^- \to \tau_{\Omega_n} \exp[-ik_n x - i\Omega_n t] \ (for\ x \to -\infty) \tag{22}$$

where $k_n = \sqrt{\Omega_n}$ and $\Omega_n = \Omega + n\omega$. $|\tau_\Omega|^2$ is the probability to penetrate the stationary barrier with energy Ω.

The boundary conditions at $x = 0$ are

$$\psi_l(0) = \psi_r(0)\ and\ \psi_l'(0) - \psi_r'(0) = -(\alpha + \beta\cos(\omega t))\psi_r(0) \tag{23}$$

where the subscripts "r" and "l" represent the wavefunction to the right and to the left of the well, respectively. Using this terminology, the dynamics can be presented with the following difference equation:

$$-\chi_n \delta(n) = (\alpha - \chi_n)s_n + \frac{\beta}{2}(s_{n+1} + s_{n-1}) \tag{24}$$

where $s_n \equiv t_n\left(\varphi_n^+ / \varphi_0^+\right)$ and $\chi_n \equiv \frac{\varphi_n^{+\prime}}{\varphi_n^+} - \frac{\varphi_n^{-\prime}}{\varphi_n^-} = \frac{1}{G_n^+(0)} \equiv -2\rho_n \tanh[\rho_n L - i\arctan(k_n/\rho_n)]$ [8,33]. $G_n^+(0)$ is the outgoing Green function of Equation (20) at $x = 0$

$$-\frac{\partial^2}{\partial x^2} G_n^+(x) + [V(x) - \Omega_n] G_n^+(x) = -\delta(x) \tag{25}$$

and $\rho_n = \sqrt{U - \Omega_n}$. Finally, the current through the barrier is

$$j = 2\Re \sum_{n=-\infty}^{\infty} |t_n|^2 |\tau_n|^2 k_n \tag{26}$$

where the abbreviation $\tau_n \equiv \tau_{\Omega_n}$ is used.

Equation (24) can be solved numerically using matrix formalism:

$$\mathbf{s} = M^{-1}\mathbf{v} \tag{27}$$

where

$$\mathbf{s} \equiv \begin{pmatrix} \vdots \\ s_{-2} \\ s_{-1} \\ s_0 \\ s_1 \\ s_2 \\ \vdots \end{pmatrix},\ M = \begin{pmatrix} \ddots & \ddots & & & & & \\ \ddots & \alpha - \chi_{-2} & \beta/2 & & & & \\ & \beta/2 & \alpha - \chi_{-1} & \beta/2 & & & \\ & & \beta/2 & \alpha - \chi_0 & \beta/2 & & \\ & & & \beta/2 & \alpha - \chi_1 & \beta/2 & \\ & & & & \beta/2 & \alpha - \chi_2 & \ddots \\ & & & & & \ddots & \ddots \end{pmatrix}\ and\ \mathbf{v} = \begin{pmatrix} \vdots \\ 0 \\ 0 \\ -\chi_0 \\ 0 \\ 0 \\ \vdots \end{pmatrix} \tag{28}$$

A zero current occurs when there are no propagating modes. This occurs when the higher half of the spectrum vanishes, i.e., $s_n = 0$ for $n \geq 0$, and the incoming particle's energy is lower than the oscillating frequency $\Omega < \omega$.

4. A Solution in the Slowly Varying Approximation

When the slowly varying approximation of the Sisyphus effect (Equation (16)) is applied to Equation (14), i.e., to the harmonically oscillating case, we find

$$\left(\Omega - U + \frac{2\alpha^2 + \beta^2}{8}\right) t_1 + \frac{\beta^2}{16\omega}\left[\sin(2\omega t_1) + 8\frac{\alpha}{\beta}\sin(\omega t_1)\right] = \pi\left(n_1 \mp \frac{1}{4}\right)$$
$$\text{where } t_1 = \frac{1}{\omega}\arccos\left(\frac{2\sqrt{U-\Omega} - \alpha}{\beta}\right) \tag{29}$$

where the $-/+$ sign corresponds to Equations (3) and (8), respectively, i.e., the minus corresponds to current suppression and the plus corresponds to current enhancement. After substituting t_1 in Equation (29), the equation can be rewritten:

$$\pi\left(n_1 \mp \tfrac{1}{4}\right) = \frac{1}{\omega}\left[\frac{\beta}{8}\left(3\alpha + 2\sqrt{U-\Omega}\right)\sqrt{1-\frac{\left(\alpha-2\sqrt{U-\Omega}\right)^2}{\beta^2}} + (\Omega - \langle\Omega_R\rangle)acos\left(\frac{2\sqrt{U-\Omega}-\alpha}{\beta}\right)\right] \tag{30}$$

since

$$\frac{1}{2}\int_{-\pi/\omega}^{\pi/\omega}\left[\Omega - U + \frac{1}{4}(\alpha + \beta\cos\omega t)^2\right]dt = \left(\frac{\alpha^2+\beta^2/2}{4} + (\Omega - U)\right)\frac{\pi}{\omega} = (\Omega - \langle\Omega_R\rangle)\frac{\pi}{\omega} \tag{31}$$

Equivalently, the same criterion applied in the second part of the period leads to

$$\pi\left(n_2 \mp \tfrac{1}{4}\right) = \frac{1}{\omega}\left[\frac{\beta}{8}\left(3\alpha + 2\sqrt{U-\Omega}\right)\sqrt{1-\frac{\left(\alpha-2\sqrt{U-\Omega}\right)^2}{\beta^2}} + (\Omega - \langle\Omega_R\rangle)\left[acos\left(\frac{2\sqrt{U-\Omega}-\alpha}{\beta}\right) - \pi\right]\right] \tag{32}$$

To simplify the expressions, let us focus on the large oscillating amplitude regime ($2\sqrt{U-\Omega} - \alpha << \beta$), since $\Omega - \langle\Omega_R\rangle << \alpha^2$ and $|\beta| << |\alpha|$ (note that α is negative); then, Equation (30) reduces to

$$(\Omega - \langle\Omega_R\rangle)\frac{\pi}{2\omega} - \frac{\alpha\beta}{2\omega} = \pi\left(n_1 \mp \frac{1}{4}\right) \tag{33}$$

and therefore, the energy must be

$$\Omega = \langle\Omega_R\rangle + \frac{\alpha\beta}{\pi} + 2\omega\left(n_1 \mp \frac{1}{4}\right) \tag{34}$$

Similarly, the suppression/enhancement criterion applied in the second part of the period (following Equation (30)) leads to

$$(\Omega - \langle\Omega_R\rangle)\frac{\pi}{2\omega} + \frac{\alpha\beta}{2\omega} = -\pi\left(n_2 \mp \frac{1}{4}\right) \tag{35}$$

and therefore the energy must be

$$\Omega = \langle\Omega_R\rangle - \frac{\alpha\beta}{\pi} - 2\omega\left(n_2 \mp \frac{1}{4}\right) \tag{36}$$

Therefore, (34) and (36) can both be valid with the same sign, provided that $\Omega = \Omega_m = \langle\Omega_R\rangle + m\omega$ and $m = n_1 - n_2$. Therefore, as was shown above, when the energy coincides with one of the energies Ω_m then the entire spectrum is suppressed or is excited.

On the other hand, when $\Omega = \Omega_{m+1/2} = \langle\Omega_R\rangle + (m+1/2)\omega$, then if one part of the spectrum is suppressed (say the lower one), then the other side (say the higher one) is excited and vice versa.

5. A Formal Derivation in the Quasi-Classical Regime

χ_n of Equation (24) in the quasi-classical approximation, i.e., $\omega << U - \Omega$, reads

$$\chi_n \cong -2\sqrt{U - \Omega_R - \Omega + \Omega_R - n\omega} \cong -2\rho_0 + (\Omega - \Omega_R + n\omega)/\rho_0 \tag{37}$$

where $\rho_0 = \sqrt{U - \Omega_R}$ and

$$\frac{4}{\beta}\rho_0\delta(n) = 2\frac{\omega}{\rho_0}\left(\frac{[\rho_0(\alpha + 2\rho_0) - \Omega + \Omega_R]/\omega - n}{\beta}\right)s_n + (s_{n+1} + s_{n-1}), \tag{38}$$

respectively. Therefore, using the notations

$$\Delta = [\rho_0(\alpha + 2\rho_0) - \Omega + \Omega_R]/\omega \text{ and } z \equiv \beta\rho_0/\omega \tag{39}$$

the solution of (38) can be written as follows:

$$s_n = \begin{cases} AJ_{n-\Delta}(\beta\rho_0/\omega) & n > 0 \\ BJ_{-n+\Delta}(\beta\rho_0/\omega) & n < 0 \end{cases} \tag{40}$$

where A and B are coefficients, and $J_\nu(z)$ are the Bessel function (see, for example, Ref. [34]). Matching the solution at n = 0 yields

$$AJ_{-\Delta}(\beta\rho_0/\omega) = BJ_{+\Delta}(\beta\rho_0/\omega) \tag{41}$$

and

$$\frac{4}{\beta}\rho_0 = (AJ_{-\Delta+1}(\beta\rho_0/\omega) - BJ_{+\Delta+1}(\beta\rho_0/\omega)) \tag{42}$$

After solving Equations (41) and (42), the final solution reads

$$s_n = \begin{cases} WJ_{+\Delta}(\beta\rho_0/\omega)J_{n-\Delta}(\beta\rho_0/\omega) & n > 0 \\ WJ_{-\Delta}(\beta\rho_0/\omega)J_{-n+\Delta}(\beta\rho_0/\omega) & n < 0 \end{cases} \tag{43}$$

where

$$W = \frac{4\rho_0/\beta}{J_{+\Delta}(\beta\rho_0/\omega)J_{-\Delta+1}(\beta\rho_0/\omega) - J_{+\Delta+1}(\beta\rho_0/\omega)J_{-\Delta}(\beta\rho_0/\omega)} \tag{44}$$

Therefore, to suppress the high energy part of the spectrum, one requires

$$J_{+\Delta}(\beta\rho_0/\omega) = 0 \tag{45}$$

and to suppress the lower part of the spectrum,

$$J_{-\Delta}(\beta\rho_0/\omega) = 0 \tag{46}$$

Clearly, Equations (45) and (46) suppress the half spectrum to zero.

In the regime where $z \equiv \beta\rho_0/\omega >> 1$, i.e., with slowly varying approximation and large oscillating amplitudes, one can use the approximation [34] $J_\nu(z) \sim \sqrt{2/(\pi z)}\cos\left(z - \frac{1}{2}\nu\pi - \frac{1}{4}\pi\right)$ to obtain equivalent expressions to (34) and (36), i.e.,

$$\frac{\beta\rho_0}{\pi} \pm \frac{1}{2}[\rho_0(\alpha + 2\rho_0) - \Omega + \langle\Omega_R\rangle] = \omega\left(m - \frac{1}{4}\right) \tag{47}$$

And again, since $2\sqrt{U - \langle\Omega_R\rangle} - |\alpha| << \beta$ and $\beta << |\alpha|$, then up to the second order of β

$$\Omega = \langle\Omega_R\rangle \pm \left[\frac{\beta\alpha}{\pi} + 2\omega\left(m - \frac{1}{4}\right)\right] \tag{48}$$

Therefore, the upper sign (+) leads to Equation (34) and the lower sign (−) leads to Equation (36). Similarly, an enhancement criterion leads to

$$\Omega = \langle\Omega_R\rangle \pm \left[\frac{\beta\alpha}{\pi} + 2\omega\left(m + \frac{1}{4}\right)\right] \tag{49}$$

where, again, the upper sign (+) leads to Equation (34) and the lower sign (−) leads to Equation (36), as should be expected.

In Figure 4, the logarithm of the coefficient $|s_n|^2$ is presented as a function of both the incoming particle's energy Ω and the spectral mode n. As can be seen, all three patterns appear. When $\Omega = \langle \Omega_R \rangle + n\omega$, then when (49) is valid, Full Spectrum Excitation (FSE) is achieved. When (48) is valid, then Full Spectrum Suppression (FSS) is reached. On the other hand, when $\Omega = \langle \Omega_R \rangle + (n + 0.5)\omega$, then when (48) is valid the Half Spectrum Suppression (HSS) is reached.

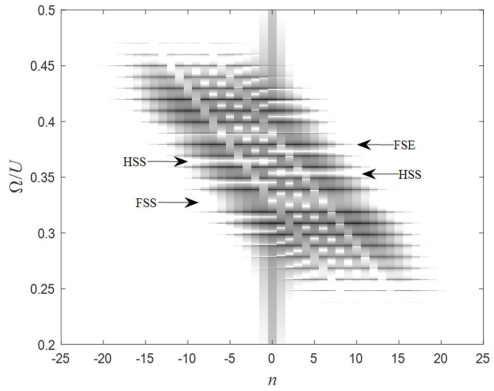


Figure 4. The logarithm of $|s_n|^2$ (solution of Equation (27)) as a function of the incoming energy and the output mode number n. Dark color designates high amplitude. FSE, FSS and HSS stand for Full Spectrum Excitation, Full Spectrum Suppression and Half Spectrum Suppression, respectively. The parameters are $LU^{1/2} = 7$, $\alpha U^{-1/2} = -1.6$, $\beta U^{-1/2} = 0.08$ and $\omega/U = 0.01009$ and the vectors (28) consist of 71 components, of which only 51 are presented.

In Figure 5, the current is presented as a function of the incoming particle's energy and the oscillation amplitude. Therefore, it presents the dependence of the current spectrum on the oscillations' amplitude. As should be expected, the spectrum widens with the corresponding increase in the amplitude. On the right panel of Figure 5, the solutions of Equations (48) and (49) are presented. The solutions of Equation (48), which are related to current suppression, are presented by red lines (solid and dashed), while the solutions of Equation (49), which are related to the current enhancement, are presented by blue lines (solid and dashed).

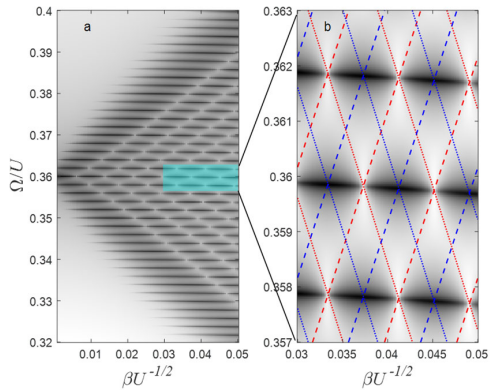


Figure 5. (**a**): The current as a function of the incoming energy and the oscillation amplitude. Dark color designates high current. The larger the amplitude the wider the QBSS spectrum, which supports a wider range of incoming energies. (**b**): An enlargement of the blue area on the left panel but with the analytical solutions of Equations (48) (red curves) and (49) (blue curves) above the numerical results. The parameters are $LU^{1/2} = 7$, $\alpha U^{-1/2} = -1.6$ and $\omega/U = 0.002$.

Despite the fact that the equations in Section 4 and Equations (48) and (49) were derived, for simplicity, in the high amplitude regime, Figure 5 shows that these equations show high agreement with numerical analysis even in the low amplitude regime.

The main results can be clearly seen: the difference between adjacent destructive and constructive solutions is ω. Two blue lines intersect when $\frac{\beta\alpha}{\pi} = -2\omega\left(m_1 + \frac{1}{4}\right)$ and two red lines intersect when $\frac{\beta\alpha}{\pi} = -2\omega\left(m_2 - \frac{1}{4}\right)$. On the other hand, a red line intersects a blue line when Equations (48) and (49) are valid, simultaneously with the opposite signs; hence, a red line intersects a blue line when $\frac{\alpha\beta}{\pi} = 2\omega m$, and the gap between adjacent similar scenarios is $\alpha\Delta\beta = 2\pi\omega$. However, Equations (48) and (49) can be valid simultaneously both when Equation (48) has a '+' sign and Equation (49) has a '$-$' sign, or when Equation (48) has a '$-$' sign and Equation (49) has a '+' sign. Both scenarios represent half-spectrum suppressions; however, the first scenario (Equation (48) with a '$-$' sign) represents the total suppression of the lower energies, and the second scenario (Equation (48) with a '+' sign) represents the suppression of the higher energies. Therefore, the gap between the two scenarios is $\alpha\Delta\beta = \pi\omega$.

In Figure 5, two red lines' intersection occurs only when the current is suppressed (see the red curves in Figures 6 and 7). Two blue line intersections occur when the current is enhanced (see the blue curves in Figures 6 and 7). As can be seen from Figures 5 and 6, in both cases the spectrum is symmetric with respect to the central energy of the spectrum, i.e., the spectrum has a similar shape for $\Omega - \langle\Omega_R\rangle = \omega$ and for $\Omega - \langle\Omega_R\rangle = -\omega$.

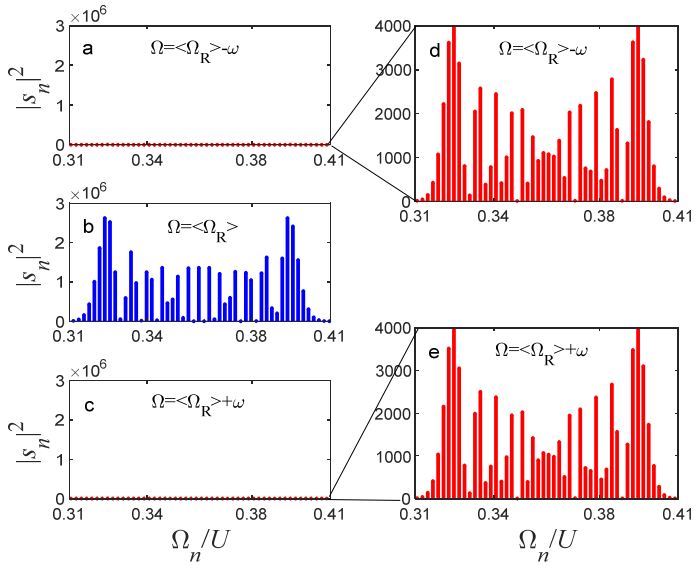


Figure 6. The same parameters as in Figure 5 but with the amplitude $\beta U^{-1/2} = 0.04909$. The output spectrum is presented for different incoming energies. (**a**) and (**c**): The current suppression criterion: Equation (48) for $\Omega = \langle\Omega_R\rangle \pm \omega$ (the intersection between the red curves in Figure 5b, i.e., destructive interference in both directions). The scenarios (**a**) and (**c**) are enlarged in (**d**) and (**e**), respectively. (**b**): The activation criterion: Equation (49), for $\Omega = \langle\Omega_R\rangle$ (the intersection between the blue curves in Figure 5b), i.e., constructive interference in both directions. Note the resemblance between the two cases: $\Omega = \langle\Omega_R\rangle \pm \omega$.

At the intersections of blue and red lines in Figure 5, the current is suppressed. In these cases, the spectrum is anti-symmetric with respect to $\langle\Omega_R\rangle$. As can be seen in Figure 8, the spectrum is flipped: for $\Omega - \langle\Omega_R\rangle = \omega/2$, the lower part of the spectrum vanishes, while for $\Omega - \langle\Omega_R\rangle = -\omega/2$ the higher part of the spectrum vanishes.

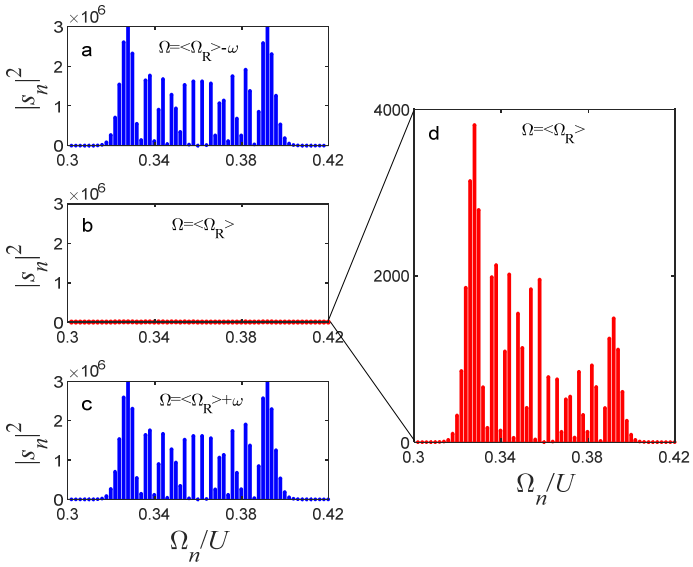


Figure 7. The same parameters as in Figure 5 but with the amplitude $\beta U^{-1/2} = 0.04516$. The output spectrum is presented for different incoming energies. (**a**) and (**c**): The activation criterion: Equation (49) for $\Omega = \langle \Omega_R \rangle \pm \omega$ (the crossing point between the blue curves in Figure 5b). (**b**) The current suppression criterion: Equation (48) for $\Omega = \langle \Omega_R \rangle$ (the crossing point between the red curves in Figure 5b). (**d**) is an enlargement of (**b**). Note the resemblance between the two cases: $\Omega = \langle \Omega_R \rangle \pm \omega$.

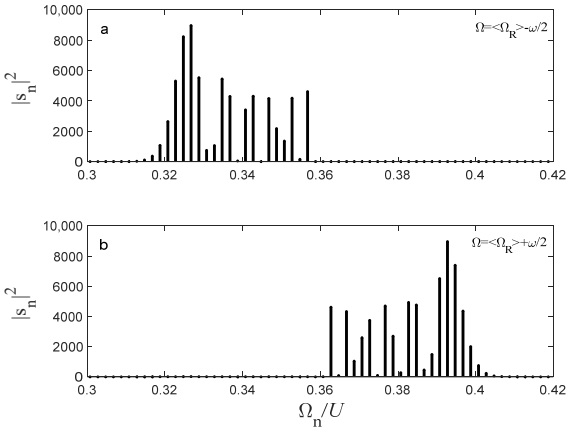


Figure 8. Same parameters as in Figure 5, for the amplitude $\beta U^{-1/2} = 0.0471$. Both Equations (48) and (49) are valid simultaneously (with opposite signs); these points are seen in the intersection of the red and blue lines in Figure 5. On the upper panel, (**a**), the incoming energy is $\Omega = \langle \Omega_R \rangle - \omega/2$ and the high energies' spectral components are suppressed, and on the bottom panel, (**b**), $\Omega = \langle \Omega_R \rangle + \omega/2$ and the lower spectral components are suppressed.

6. Half-Spectrum Suppression Leads to 100% Reflection and Fano Resonance

In Figure 5, the currents in the suppression scenarios are not much different between the different types of suppressions, and the differences between the spectra do not have much influence on the current. However, in the case where the incoming particle's energy is lower than the oscillations' frequency $\Omega < \omega$, then in the case of suppression of the upper half of the spectrum all the positive spectral components vanish, and the transmission reaches zero. These zero-transmissions/Fano-resonances are marked by black arrows in Figure 9 for the case $\Omega < \omega$. The spectral components at these resonances consist of only negative energies (see, for example, the black spectrum in Figure 10).

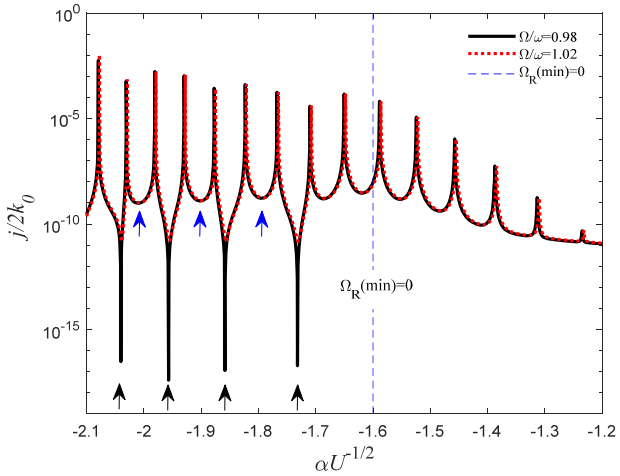


Figure 9. The current as a function of α for adjacent incoming energy. In the black curve, the incoming energy is slightly lower than the oscillations' frequency $\Omega < \omega$. The black arrows represent the cases when the higher energies of the spectrum (i.e., $\Omega_{out} \geq \Omega$) are suppressed, and since there are no positive energies that can propagate, a 100% reflection appears. The blue arrows represent the case when the lower part of the spectrum (i.e., $\Omega_{out} < \Omega$) is suppressed; in that case, there are positive energies with a finite probability to escape from the well out through the barrier, and therefore the suppression is not complete. The dotted red curve represents the case where the incoming energy is slightly higher than the frequency $\Omega > \omega$; in this case, there is always a spectral component with positive energy, and therefore a total reflection cannot exist. The parameters are $LU^{1/2} = 7$, $\beta U^{-1/2} = 0.4$ and $\omega = 0.05$.

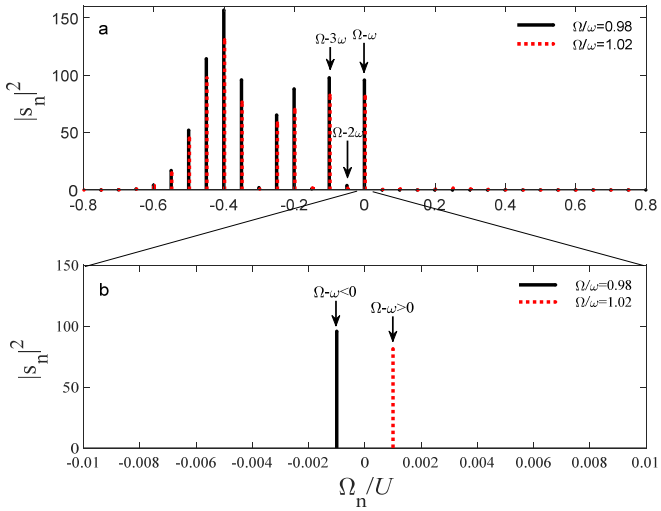


Figure 10. Here, (**b**) is an enlargement of (**a**). The parameters are as in Figure 9 for the case of $\alpha U^{-1/2} = -2.04$. This scenario is represented by the left-most black arrow in Figure 9. The high-energies part of the spectrum is suppressed for both incoming energies, but although both spectra are very similar, they lead to fundamentally different scenarios. For the case of $\Omega/\omega < 1$ (black curve in Figures 9 and 10), there are no positive spectral components; in that case, 100% reflection occurs, as can be seen in Figure 9. On the other hand, for the case $\Omega/\omega > 1$ (dotted red curve in Figures 9 and 10), there is a single spectral component with positive energy (**b**). This minor difference is sufficient to prevent a total reflection since this positive spectral component has a finite probability of escaping from the varying well out through the barrier.

In Figure 9, the current is presented as a function of α for two adjacent incoming energies, $\Omega < \omega$ (black curve) and $\Omega > \omega$ (dotted red curves). Around the blue arrows, there is not much difference between suppressions in both cases ($\Omega < \omega$, $\Omega > \omega$); the

reason is that the lower part of the spectrum is suppressed and the other part of the spectrum consists of positive energies with finite probability to tunnel out of the barrier (see Figure 11). On the other hand, around the black arrows, the difference between the suppressions in the two scenarios is fundamental. For the case $\Omega < \omega$ (black curve), the current reaches zero since the high spectral components are suppressed and all the remaining spectral components are negative $(\Omega - n\omega) < 0$, $n = 1, 2 \ldots$ (see Figure 10). However, for the case of $\Omega > \omega$ (dotted red curve), although the high spectral components are suppressed, there is still a component (or components) with positive energy, $\Omega - n\omega > 0$, and therefore with a finite probability to escape and tunnel out of the barrier. In Figure 10, the spectra are presented for the case marked by the left black arrow in Figure 9. Although the difference between the incoming energies is very minor, and although the spectra are almost identical, for the case $\Omega > \omega$ (dotted red curve) there is a single component ($n = 1$) with positive energy $\Omega - \omega > 0$ (see Figure 10b). This minor difference is sufficient to prevent a total reflection since the positive spectral component has a finite probability of escaping from the varying well out through the barrier. Although the current does not reach zero for the case $\Omega > \omega$ (dotted red curve), the black arrows' region is lower than the one marked with blue arrows, the reason is that there are fewer remaining spectral components (or even a single component) with positive energies, and those remaining components obviously have low energies, $\Omega - n\omega < \Omega$, which have a lower probability to tunnel through the barrier.

It should be noted that the spectral width of the Fano resonances, i.e., the zero transmission region, is proportional to β^2 but also depends on the order of the resonance (see Ref. [8]).

It should be noted that in cases where the minimum instantaneous resonant energy is negative and the incoming particle's energy matches one of the QBSS energies, i.e., $\Omega = \langle \Omega_R \rangle + n\omega$, then only the '$-$' sign (in Equation (48)) is valid, and in this case the upper half of the spectrum vanishes. Therefore, if, in addition, the incoming particle's energy is lower than the oscillation frequency $\Omega < \omega$, a total reflection occurs.

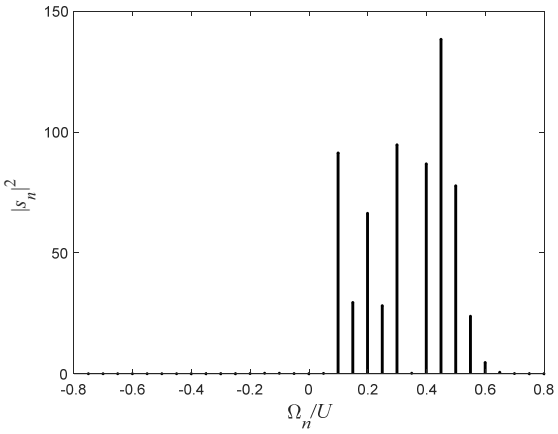


Figure 11. The parameters are as in Figure 9 for $\Omega/\omega = 0.98$ and $\alpha U^{-1/2} = -1.79$. This scenario is represented by the far-right blue arrow in Figure 9. The lower part of the spectrum is suppressed; therefore, all the spectral components are positive and there is a finite probability of escaping from the varying well and tunneling out through the barrier. In that case, the transmission is suppressed; however, it cannot reach zero.

7. Summary

It has been shown before that, in a dynamic resonant tunneling system, the tunneling current is highly suppressed when a QR (3) holds. Moreover, it has been shown that the varying well generates a QBSS, which consists of multiple interconnected quasi-states.

Current suppression occurs even when the incoming particle's energy agrees with the QBSS spectral components. However, it has been shown in this paper that, in these cases, despite current suppression, the current cannot vanish. To achieve zero current, the

energy must be between two spectral components of the QBSS. Furthermore, it is shown that the difference in current suppression is accompanied by fundamental changes in the current's spectra; when the energy agrees with the QBSS spectral components, then the entire spectrum is suppressed uniformly. However, when the particle's energy is in between the QBSS spectral components, then the spectrum is split. Half the spectrum vanishes. Then, if the half that vanishes is the upper one, and the incoming particle's energy is lower than the oscillating frequency, the current vanishes completely.

Author Contributions: Writing—original draft preparation, G.Z. and E.G.; investigation, G.Z. and E.G.; formal analysis, G.Z. and E.G. All authors have read and agreed to the published version of the manuscript.

Funding: This research received no external funding.

Institutional Review Board Statement: Not applicable.

Informed Consent Statement: Not applicable.

Data Availability Statement: The data presented in this study are available in the article.

Conflicts of Interest: The authors declare no conflict of interest.

References

1. Grossmann, F.; Dittrich, T.; Jung, P.; Hanggi, P. Coherent destruction of tunneling. *Phys. Rev. Lett.* **1991**, *67*, 516. [CrossRef] [PubMed]
2. Grossmann, F.; Hiinggi, P. Localization in a driven two-level dynamics. *Europhys. Lett.* **1992**, *18*, 571. [CrossRef]
3. Lin, W.A.; Ballentine, L.E. Quantum tunneling and chaos in a driven anharmonic oscillator. *Phys. Rev. Lett.* **1990**, *65*, 2927. [CrossRef]
4. Lin, W.A.; Ballentine, L.E. Quantum tunneling and regular and irregular quantum dynamics of a driven double-well oscillator. *Phys. Rev. A* **1992**, *45*, 3637. [CrossRef]
5. Kayanuma, Y. Role of phase coherence in the transition dynamics of a periodically driven two-level system. *Phys. Rev. A* **1994**, *50*, 843. [CrossRef] [PubMed]
6. Kayanuma, Y. Stokes phase and geometrical phase in a driven two-level system. *Phys. Rev. A* **1997**, *55*, 2495. [CrossRef]
7. Bagwell, P.F.; Lake, R.K. Resonances in transmission through an oscillating barrier. *Phys. Rev. B* **1992**, *46*, 15329. [CrossRef]
8. Zangwill, G.; Granot, E.E. Multiple Fano resonances in dynamic resonant tunneling processes. *Appl. Sci.* **2023**, *13*, 6767. [CrossRef]
9. Chynoweth, A.G.; Logan, R.A.; Thomas, D.E. Phonon-assisted tunneling in silicon and germanium Esaki junctions. *Phys. Rev.* **1962**, *125*, 877. [CrossRef]
10. Fujisawa, T.; Tarucha, S. Photon assisted tunneling in single and coupled quantum dot systems. *Superlattices Microstruct.* **1997**, *21*, 247. [CrossRef]
11. Shchurova, L.Y.; Murzin, V.N. Phonon-Assisted Tunneling Current in a Double-Barrier Heterostructure with a Quantum Well. *J. Russ. Laser Res.* **2021**, *42*, 632–642. [CrossRef]
12. Vdovin, E.E.; Mishchenko, A.; Greenaway, M.T.; Zhu, M.J.; Ghazaryan, D.; Misra, A.; Cao, Y.; Morozov, S.V.; Makarovsky, O.; Fromhold, T.M.; et al. Phonon-assisted resonant tunneling of electrons in graphene boron nitride transistors. *Phys. Rev. Lett.* **2016**, *116*, 186603. [CrossRef] [PubMed]
13. Kot, P.; Drost, R.; Uhl, M.; Ankerhold, J.; Cuevas, J.C.; Ast, C.R. Microwave-assisted tunneling and interference effects in superconducting junctions under fast driving signals. *Phys. Rev. B* **2020**, *101*, 134507. [CrossRef]
14. Platero, G.; Aguado, R. Photon-assisted transport in semiconductor nanostructures. *Phys. Rep.* **2004**, *395*, 1. [CrossRef]
15. Kohler, S.; Lehmann, J.; Hänggi, P. Driven quantum transport on the nanoscale. *Phys. Rep.* **2005**, *406*, 379. [CrossRef]
16. Azbel, M.Y. Elevator resonance activation. *Europhys. Lett.* **1992**, *18*, 537. [CrossRef]
17. Azbel, M.Y. Eigenstate Assisted Activation. *Phys. Rev. Lett.* **1992**, *68*, 98. [CrossRef]
18. Zangwill, G.; Granot, E. Eigenstate suppressed activation. *Physica B* **2015**, *461*, 140. [CrossRef]
19. Granot, E. Selected elevation in quantum tunneling. *Europhys. Lett.* **2003**, *61*, 817. [CrossRef]
20. Wagner, M. Quenching of resonant transmission through an oscillating quantum well. *Phys. Rev. B* **1994**, *49*, 16544. [CrossRef]
21. Wagner, M. Photon-assisted transmission through an oscillating quantum well: A transfer-matrix approach to coherent destruction of tunneling. *Phys. Rev. A* **1995**, *51*, 798. [CrossRef] [PubMed]
22. Zangwill, G.; Granot, E. Dynamic resonant tunneling via a quasibound superstate. *Phys. Rev. A* **2022**, *106*, 032201. [CrossRef]
23. Granot, E.; Zangwill, G. Generic temporal quantization criterion in dynamic resonant tunneling for current suppression. *Physica B* **2023**, *669*, 415332. [CrossRef]
24. Tekman, E.; Bagwell, P. Fano resonances in quasi-one-dimensional electron waveguides. *Phys. Rev. B* **1993**, *48*, 2553. [CrossRef] [PubMed]

25. Ueda, A.; Eto, M. Resonant tunneling and Fano resonance in quantum dots with electron-phonon interaction. *Phys. Rev. B* **2006**, *73*, 235353. [CrossRef]
26. Miroshnichenko, A.E.; Flach, S.; Kivshar, Y.S. Fano resonances in nanoscale structures. *Rev. Mod. Phys.* **2010**, *82*, 2257. [CrossRef]
27. Thuberg, D.; Reyes, S.A.; Eggert, S. Quantum resonance catastrophe for conductance through a periodically driven barrier. *Phys. Rev. B* **2016**, *93*, 180301. [CrossRef]
28. Briones-Torres, J.A.; Rodriguez-Vargas, I. Fano resonances in bilayer graphene superlattices. *Sci. Rep.* **2017**, *7*, 16708. [CrossRef]
29. Cocklin, S.; Morr, D.K. Scanning tunneling shot noise spectroscopy in Kondo systems. *Phys. Rev. B* **2019**, *100*, 125146. [CrossRef]
30. Biswas, R.; Sinha, C. Quenching effect of oscillating potential on anisotropic resonant transmission through a phosphorene electrostatic barrier. *Sci. Rep.* **2021**, *11*, 2881. [CrossRef]
31. Ben-Asher, A.; Šimsa, D.; Uhlí, T.; Šindelka, M.; Moiseyev, N. Laser Control of Resonance Tunneling Via an Exceptional Point. *Phys. Rev. Lett.* **2020**, *124*, 253202. [CrossRef] [PubMed]
32. Landau, L.D.; Lifschitz, E.M. *Quantum Mechanics*; Sec 46; Pergamon: Oxford, UK, 1976.
33. Merzbacher, E. *Quantum Mechanics*; Wiley: New York, NY, USA, 1970.
34. Abramowitz, M.; Stegun, A. *Handbook of Mathematical Functions*; Dover Publications: New York, NY, USA, 1965.

Disclaimer/Publisher's Note: The statements, opinions and data contained in all publications are solely those of the individual author(s) and contributor(s) and not of MDPI and/or the editor(s). MDPI and/or the editor(s) disclaim responsibility for any injury to people or property resulting from any ideas, methods, instructions or products referred to in the content.